ORGANOMETALLICS

Article

pubs.acs.org/Organometallics

Diamido-Ether Actinide Complexes as Catalysts for the Intramolecular Hydroamination of Aminoalkenes

Cassandra E. Hayes,[†] Rachel H. Platel,[‡] Laurel L. Schafer,*[,‡] and Daniel B. Leznoff*[,†]

[†]Department of Chemistry, Simon Fraser University, 8888 University Drive, Burnaby, British Columbia V5A 1S6, Canada

[‡]Department of Chemistry, University of British Columbia, 2036 Main Mall, Vancouver, British Columbia V6T 1Z1, Canada

Supporting Information

ABSTRACT: The synthesis and characterization of a series of new diamido-thorium(IV) and diamido-uranium(IV) halide and alkyl complexes supported by three different diamido-ether ligands are reported. Reaction of $ThCl_4$·2DME with $[(RNSiMe_2)_2O]Li_2$ ($[^{R}NON]Li_2$) in DME when R = ^{t}Bu gives $[^{tBu}NON]ThCl_5Li_3$·DME (**1**), when R = $^{i}Pr_2Ph$ in diethyl ether $[^{iPr_2Ph}NON]ThCl_3Li$·DME (**3**) is prepared. Reaction of UCl_4 with $[^{iPr_2Ph}NON]Li_2$ in diethyl ether gives $\{[^{iPr_2Ph}NON]UCl_2\}_2$ (**4**). Reaction of $ThCl_4$·2DME with $Li_2[(^{i}Pr_2PhNCH_2CH_2)_2O]$ ($[^{iPr_2Ph}NCOCN]Li_2$) in DME gives $[^{iPr_2Ph}NCOCN]ThCl_2$·DME (**5**). The addition of 2 equiv of $LiCH_2SiMe_3$ to **1** and **5** resulted in salt- and base-free $[^{tBu}NON]Th(CH_2SiMe_3)_2$ (**7**) and $[^{iPr_2Ph}NCOCN]Th(CH_2SiMe_3)_2$ (**9**), respectively. Complexes **1**, **3**, **4**, **7**, and **9**, as well as previously reported $\{[^{tBu}NON]UCl_2\}_2$ (**2**), $[^{tBu}NON]U(CH_2SiMe_3)_2$ (**6**), and $[^{iPr_2Ph}NCOCN]U(CH_2SiMe_3)_2$ (**8**) were examined as catalysts for the intramolecular hydroamination of a series of aminoalkenes. Complexes **6**−**9** were shown to facilitate the formation of 2-methyl-4,4-diphenylpyrrolidine from 2,2-diphenyl-1-amino-4-pentene at room temperature. For **9**, this reaction occurs in less than 15 min, while for other dialkyls **6**−**8**, the reaction takes less than 2 h. Dihalides **1** and **2** facilitated the same reaction at 60 °C in 4 h, while **3** and **4** showed no activity under the same conditions. Dialkyl complexes **7**−**9** were examined for further reactivity with different substrates. The uranium dialkyl **8** was more active than **7** and **9** for the cyclization of 2,2-diphenyl-1-amino-5-hexene and 2,2-diphenyl-1-amino-6-heptene, as well as more active in the cyclization of *N*-methyl-2,2-diphenyl-1-amino-4-pentene, a secondary amine. All three dialkyls became less active when the steric bulk of the *gem*-substituents was decreased from diphenyl to cyclopentyl; reactivity further decreased when the steric bulk of the substituents was decreased further to hydrogen.

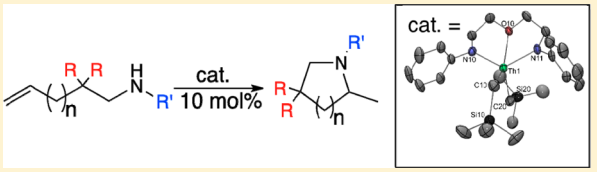

INTRODUCTION

Catalytic hydroamination, the formal addition of an N−H bond across a multiple C−C bond, provides an atom economical route to complex nitrogen-containing organic molecules that have numerous pharmaceutical and industrial applications.[1−5] Research into catalysts that are capable of facilitating this reaction is widespread, and a huge number of early[6−19] and late transition metal[20−30] and lanthanide[31−40] catalysts have been reported in the literature in recent years. In contrast, there are fewer examples of actinide complexes that mediate hydroamination reactions.[41−50] Compared to lanthanides, the actinides offer a unique set of characteristics potentially useful in catalysis, namely increased coordinative unsaturation and the possibility of f-orbital participation in bonding and reactivity, as well as access to a number of oxidation states.[31,51−53]

Within the small number of actinide complexes reported to catalyze hydroamination reactions, the majority are cyclopentadienyl-based systems. For example, the intermolecular hydroamination of terminal alkynes with aliphatic primary amines, catalyzed by $Cp^*_2AnMe_2$ species (An = Th, U),[41,43] has been reported, in which a variety of terminal alkynes reacted with aliphatic primary amines to form the corresponding enamines, imines, or alkylated amines, but the reaction did not occur with secondary amines. In many cases, alkyne dimerization was a competitive process, which was unsurprising because the $Cp^*_2AnMe_2$ species have also been reported to be efficient catalysts for this process.[42,54,55] A cationic $[U(NEt_2)_3][BF_4]$ species was also developed, which was also active for the intermolecular hydroamination of terminal alkynes with primary amines, but again, alkyne dimerization was a competing process.[44] Similarly, constrained geometry actinide complexes of the form $[CGC]An(NR_2)_2$ ([CGC] = constrained geometry catalyst ligand, containing one C_5Me_4 moiety and one amide group; An = U, Th)[41,43,45−47,56,57] were designed and the activity of these species for intramolecular hydroamination reactions of primary and secondary aminoalkenes and aminoalkynes, aminodienes, and aminoallenes[46] was reported; a detailed mechanistic investigation was also conducted, presenting evidence for a σ-bond insertion mechanism.[47]

These reports of Cp-based actinide catalysts indicate that such complexes are capable of and are in many cases very active for intra- and intermolecular hydroamination reactions. By comparison, amido-based actinide complexes have been studied for this reaction in much less detail despite initial reports that amido−actinide complexes can activate a range of organic

Received: May 15, 2012
Published: September 26, 2012

molecules including those that contain C−H bonds,[55−57] C−O bonds,[58−61] as well as C−N bonds and N_2.[62−64] To our knowledge only one example of a diamido-actinide complex, a uranium dibenzyl complex supported by a diamido-ferrocene ligand, has been reported to be an efficient hydroamination catalyst.[48] A range of substrates was investigated in this study, including the intramolecular cyclization of primary and secondary aminoalkenes as well as a primary aminoalkyne and a range of intermolecular reactions involving aniline and terminal alkyne substrates. By exploring both intra- and intermolecular variants of the reaction, the aim was to determine if just one mechanism operates for each type of reaction. However, the results were inconclusive, showing that the mechanism of reaction for these systems is not simple. On the other hand, this report highlighted the application of diamido-actinide complexes toward intramolecular hydroamination catalysis with a range of aminoalkene substrates.

Herein we report the synthesis and characterization of a series of diamido-actinide complexes supported by a silyl-ether and alkyl-ether framework that are capable of intramolecular hydroamination reactions. The difference in choice of actinide metal (Th(IV) vs U(IV)) as well as the difference in the choice of diamido ligand (changes in the backbone structure and choice of amido R-group) is examined. The substrate scope of the reaction has also been explored using the most catalytically active compounds to further understand the scope of reactivity of these complexes.

RESULTS AND DISCUSSION

Synthesis of New Diamido-Actinide Halide Complexes. Diamido-actinide halide complexes **1**−**5** were prepared by a series of salt metathesis reactions with $ThCl_4$·2DME or UCl_4 and the appropriate dilithiated ligand. Thus, addition of a solution of $[(^{t\mathrm{Bu}}NSiMe_2)_2O]Li_2$ ($[^{t\mathrm{Bu}}NON]Li_2$) in DME to a solution of $ThCl_4$·2DME gave, after stirring and workup, a beige powder of $[^{t\mathrm{Bu}}NON]ThCl_5Li_3$·DME (**1**) in 62% yield. The elemental analysis of **1** has %CHN values that are considerably lower than the putative salt-free product "$[^{t\mathrm{Bu}}NON]ThCl_2$" and repeated filtration of **1** from toluene solvent does not show any change in the elemental analyses, indicating the retention of considerable LiCl in **1**. The ^{1}H NMR spectrum of **1** in THF-d_8 further supports "ate" complex formation: two resonances for inequivalent $SiMe_2$ groups at 0.89 and 1.15 ppm (indicating a reduced-symmetry system typical of ate-complexes) were observed as well as remaining, bound DME after the product has been rinsed multiple times with pentane and dried *in vacuo* overnight. Despite our inability to obtain X-ray quality crystals of **1**, it is clear that the desired "$[^{t\mathrm{Bu}}NON]ThCl_2$" fragment exists in **1** because alkylation with 2 equiv of $LiCH_2SiMe_3$ results in the clean formation of $[^{t\mathrm{Bu}}NON]Th(CH_2SiMe_3)_2$ (**7**), a previously reported salt-free diamido-thorium dialkyl complex.[65]

Similarly, addition of a solution of $[^{i\mathrm{Pr}_2\mathrm{Ph}}NON]Li_2$ in diethyl ether to a slurry of $ThCl_4$·2DME gave, after stirring and workup, a yellow−orange powder of $[^{i\mathrm{Pr}_2\mathrm{Ph}}NON]ThCl_3Li$·DME (**3**) in 48% yield. The ^{1}H NMR spectrum of **3** has 10 overlapping resonances in total, including four separate resonances for the four *iso*-propyl methyl groups and two resonances for the DME ligand coordinated to the metal. The existence of multiple resonances for the *iso*-propyl methyl groups is consistent with hindered rotation around the amido-*N* aryl bond and indicates that the "ate" complex persists in solution. The elemental analysis is also consistent with this overall formulation.

Addition of a solution of $[^{i\mathrm{Pr}_2\mathrm{Ph}}NON]Li_2$ in diethyl ether to a suspension of UCl_4 gave an orange−brown solution that after workup resulted in a brown powder of $\{[^{i\mathrm{Pr2Ph}}NON]UCl_2\}_2$ (**4**). Crystals of **4** suitable for X-ray diffraction were grown by slow evaporation of a toluene solution. The crystal structure shows a dinuclear structure with each uranium in a six-coordinate, distorted octahedral environment, coordinated by the facially bound $[^{i\mathrm{Pr}_2\mathrm{Ph}}NON]$ ligand, two bridging chloride ligands, and one terminal chloride ligand per uranium (Figure 1), as has been observed for the slightly less sterically

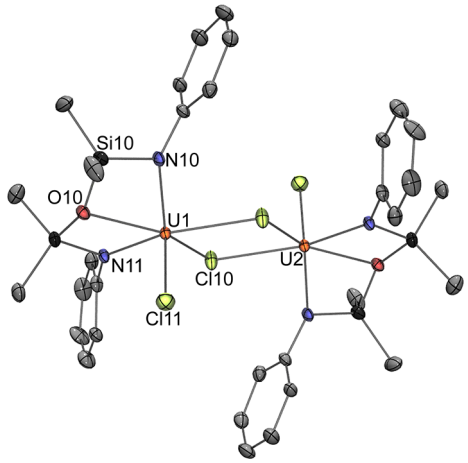

Figure 1. The molecular structure and numbering scheme for **4** (thermal ellipsoids shown at 30% probability). Hydrogen atoms and disordered toluene solvate omitted, ^{i}Pr$_2$Ph-N groups simplified for clarity. Selected bond lengths (Å) and angles (deg): U1−N10, 2.224(8); U1−N11, 2.223(8); U1−O10, 2.567(7); U1−Cl10, 2.754(3); U1−Cl11, 2.561(3); U1···U2, 4.4494(4); N10−U1−N11, 115.4(3); Cl10−U1−Cl10′, 73.93(8); N10−U1−O10, 63.3(2); N10−U1−Cl11, 105.2(2).

demanding $\{[^{t\mathrm{Bu}}NON]AnCl_2\}$ (An = Th, U).[65] The U(1)−N(10) and U(1)−N(11) bond lengths of 2.224(8) and 2.223(8) Å, respectively, are slightly longer than the U−N bonds in $\{[^{t\mathrm{Bu}}NON]UCl_2\}_2$ (**2**) (U−N 2.145(16) and 2.130(18) Å) and $[^{i\mathrm{Pr}_2\mathrm{Ph}}NCOCN]UCl_3Li$·2THF (U−N 2.183(15) and 2.192(15) Å).[65,66] The U(1)−O(10) length of 2.567(7) Å is also longer than the U−O distances in these other compounds by 0.1 Å on average. However, the terminal U(1)−Cl(11) distance of 2.561(3) Å in **4** is shorter than the terminal U−Cl distance in the diamido-amine complex $\{[^{\mathrm{SiMe}_3}NNN]UCl_2\}_2$ (2.638(1) Å) and is also shorter than the two terminal U−Cl distances in $\{[(SiMe_3)_2N]_2UCl_2$·DME$\}$ (2.630 (3) and 2.640(3) Å).[67,68] The bridging U(1)−Cl(10) distance of 2.754(3) Å is shorter than the bridging U−Cl distance of 2.811(1) Å in $\{[^{\mathrm{SiMe}_3}NNN]UCl_2\}_2$ and the bridging U−Cl distance of 2.8813(17) Å in the tripodal $[\{HC(SiMe_2NAr)_3\}UCl(\mu\text{-}Cl)U(THF)_2\{ArNSiMe_2)_3CH\}]$.[68,69] As with other bimetallic diamido-uranium complexes such as $\{[^{t\mathrm{Bu}}NON]U(CH(SiMe_3)(SiMe_2CH_2))\}_2$ (where U(1)···U(2) is 3.965(2) Å), the U(1)···U(2) distance of 4.449 Å in **4** is too long for any metal−metal interactions to be present.[70]

The ^{1}H NMR spectrum of **4** indicates a number of strongly shifted, broad resonances, typical of paramagnetic complexes. At room temperature, the spectrum portrays at least 18 overlapping resonances: four resonances for the $CH(CH_3)_2$

dx.doi.org/10.1021/om300410h | *Organometallics* 2012, 31, 6732−6740

hydrogens, four resonances for $Si(CH_3)_2$, and 10 resonances for the aryl C−*H* and methine $CH(CH_3)_2$ groups. These assignments are consistent with a low symmetry complex in solution, indicating that the dimeric structure remains in solution. Variable temperature NMR studies between 0 and 85 °C show that all of these resonances move toward the diamagnetic region but do not fully separate or coalesce, preventing any further useful assignment of the resonances.

Addition of a solution of [$^{i\mathrm{Pr}_2\mathrm{Ph}}$NCOCN]$Li_2$ in diethyl ether to a slurry of $ThCl_4$·2DME generated an orange powder of [$^{i\mathrm{Pr}_2\mathrm{Ph}}$NCOCN]$ThCl_2$·DME (**5**) in 97% yield. Orange, block-shaped crystals of **5** suitable for X-ray diffraction were grown by slow evaporation of a DME/toluene solution. The structure contains one thorium center in a seven-coordinate, distorted pentagonal bipyramidal geometry meridionally coordinated by the tridentate [$^{i\mathrm{Pr}_2\mathrm{Ph}}$NCOCN] ligand and the DME molecule in the pentagonal plane, while two chloride ligands occupy the apical positions (Figure 2). The Th(1)−N(10) and Th(1)−N(11) bond lengths of 2.327(3) and 2.319(3) Å, respectively, are unremarkable, comparing well with the Th−N lengths of 2.305(9) and 2.321(8) Å for [BDPP]$ThCl_2$·DME (BDPP = 2,6-bis(2,6-di-*iso*-propylanilidomethyl)pyridine) and Th−N lengths of 2.29(2) and 2.291(19) Å for {[$^{t\mathrm{Bu}}$NON]$ThCl_2$}$_2$.[65,71] The Th(1)−O(10) length of 2.499(3) Å is marginally shorter than in {[$^{t\mathrm{Bu}}$NON]$ThCl_2$}$_2$ (2.531(17) Å). The bound DME molecule displays a Th(1)−O(1) distance of 2.662(3) Å, which is long for a Th−O bond but compares well with other Th−DME complexes such as the Th−O distance of 2.674(8) Å for [BDPP]$ThCl_2$·DME.[71] The Cl−Th−Cl angle is 165.06(4)°, indicating some distortion from the ideal 180°; all angles in the pentagonal plane are between 59.50(10)° and 85.64(11)°.

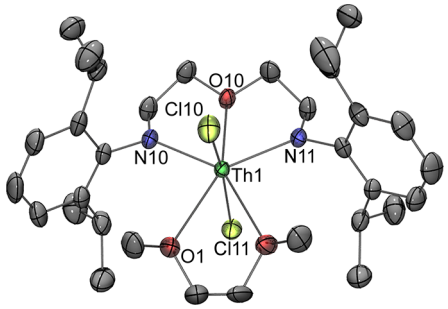

Figure 2. Molecular structure and numbering scheme of **5** (thermal ellipsoids shown at 30% probability). Hydrogen atoms are omitted for clarity. Selected bond lengths (Å) and angles (deg): Th1−N10, 2.327(3); Th1−N11, 2.319(3); Th1−O10, 2.499(3); Th1−Cl10, 2.6891(13); Th1−Cl11, 2.7443(11): Th1−O1, 2.662(3); Th1−O2, 2.675(3); N10−Th1−N11, 129.80(12); Cl10−Th1−Cl11, 165.06(4); O1−Th1−O2, 59.50(10); N10−Th1−O10, 64.67(11); N10−Th1−O1, 85.64(11).

The ^{1}H NMR spectrum of **5** has nine distinct resonances, consistent with a C_{2v} symmetric structure in solution. Two doublets are assignable to the $CH(CH_3)_2$ protons at 1.06 and 1.32 ppm, while for the corresponding $CH(CH_3)_2$, there is only one septet resonance at 4.19 ppm. This is consistent with slow rotation around the amido-N aryl bond. The $^{13}C\{^1H\}$ NMR data further supports these observations: two resonances for the methyl $CH(CH_3)_2$ groups are seen at 24.31 and 28.39 ppm and only one resonance for the secondary $CH(CH_3)_2$ carbon at 24.50 ppm is observed. As with **1**, attempts to dry the product *in vacuo* overnight resulted in no change in the Th-bound DME resonances, consistent with the observation that the DME-coordinated adduct in **5** remains intact in toluene.

Synthesis of Diamido−Actinide Dialkyl Complexes. Alkylation of the diamido-thorium dichlorides **1** and **5** proceeds via salt metathesis (Scheme 1). Thus, addition of 2 equiv of $LiCH_2SiMe_3$ to a slurry of **1** in hexanes generated a deep-yellow oil of [$^{t\mathrm{Bu}}$NON]$Th(CH_2SiMe_3)_2$ (**7**) in 83% yield; this previously reported product was originally synthesized from DME-free {[$^{t\mathrm{Bu}}$NON]$ThCl_2$}$_2$.[65] In this case, despite using the DME-solvated starting material, salt and solvent-free dialkyl products were still obtained.

Scheme 1. Synthesis of Diamido−Thorium Dialkyl Complexes 7 and 9

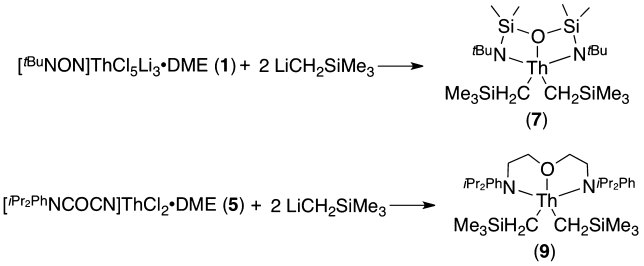

Addition of a range of alkyl lithium reagents to **3** and **4** gave an unidentifiable product that was not the desired actinide dialkyl species. Characterization of this product is ongoing, and additional attempts to alkylate **3** and **4** were unsuccessful and were not further pursued.

However, addition of 2 equiv of $LiCH_2SiMe_3$ to a slurry of **5** in hexanes gave, after 18 h and workup, an orange powder of [$^{i\mathrm{Pr}_2\mathrm{Ph}}$NCOCN]$Th(CH_2SiMe_3)_2$ (**9**) in 92% yield. Single crystals of **9** suitable for X-ray diffraction were grown by slow evaporation of a hexanes solution. Dialkyl **9** is isostructural and isomorphous with the previously reported [$^{i\mathrm{Pr}_2\mathrm{Ph}}$NCOCN]U-$(CH_2SiMe_3)_2$ (**8**), containing a five-coordinate geometry around the thorium center (Figure 3) that is coordinated by the [$^{i\mathrm{Pr2Ph}}$NCOCN] ligand as well as two η^1-CH_2SiMe_3 substituents. The Th(1)−N(10) and Th(1)−N(11) bond lengths of 2.275(5) and 2.285(5) Å, respectively, are shorter than in **5**, while the Th(1)−O(10) distance of 2.595(5) Å is

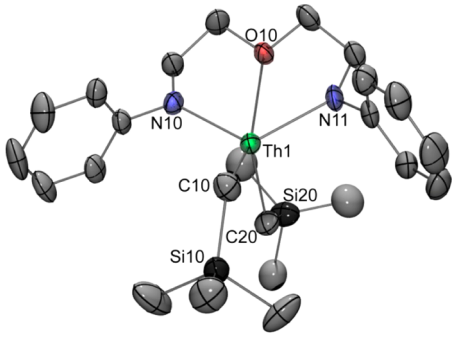

Figure 3. Molecular structure and numbering scheme for **9** (thermal ellipsoids shown at 30% probability). Hydrogen atoms omitted and ^{i}Pr$_2$Ph-N groups simplified for clarity. Selected bond lengths (Å) and angles (deg): Th1−N10, 2.275(5); Th1−N11, 2.285(5); Th1−O10, 2.595(5); Th1−C10, 2.513(8); Th1−C20, 2.490(7); C10−Si10, 1.820(8); C20−Si20, 1.845(8); N10−Th1−N11, 125.9(2); N10−Th1−O10, 64.51(17); N10−Th1−C10, 107.6(2); C10−Th1−C20, 109.7(2); Th1−C10−Si10, 125.7(4); Th1−C20−Si20, 127.1(4).

dx.doi.org/10.1021/om300410h | *Organometallics* 2012, 31, 6732−6740

longer than in **5**. These distances are comparable with the only other structurally characterized diamido-thorium dialkyl complex: ([XA_2]Th(CH_2SiMe_3)$_2$ (XA = 4,5-bis(2,6-di-*iso*-propylanilido)-2,7-di-*tert*-butyl-9,9-dimethylxanthene), which has Th−N distances of 2.292(4) and 2.312(4) Å).[71] The Th(1)−C(10) and Th(1)−C(20) lengths in **9** are 2.513(8) and 2.490(7) Å, respectively, and also compare well with those in [XA_2]Th(CH_2SiMe_3)$_2$, which has Th−C bond lengths of 2.468(6) Å and 2.485(6) Å.[71] The Th−C bond lengths in **9** are also consistent with other thorium dialkyl complexes such as [$Me_2Si(C_5Me_4)_2$]Th(CH_2SiMe_3)$_2$ (Th−C 2.54(2) and 2.48(2) Å)[72] and [Cp*]$_2$Th(CH_2SiMe_3)$_2$ (Th−C 2.47(3) and 2.44(3) Å).[73] Similar to [XA_2]Th(CH_2SiMe_3)$_2$ and [Cp*]$_2$Th(CH_2SiMe_3)$_2$, the Th−C−Si bond angles in **9** are 125.7(4)° and 127.1(4)° and are considerably larger than the expected 109.5° for an sp^3-hybridized carbon.

The ^{1}H NMR spectrum of **9** has eight distinguishable resonances, consistent with a C_s symmetric structure. As with **5**, some hindered rotation of the ^{i}Pr$_2$Ph-N groups in **9** is observed: two doublets corresponding to the CH(CH_3)$_2$ methyl protons at 1.22 and 1.49 ppm are observed as well as one C*H*(CH_3)$_2$ methyne resonance as a multiplet at 3.64 ppm. The 2D ^{1}H−^{13}C HSQC spectrum clarifies that the multiplet in the ^{1}H spectrum correlates to two overlapping carbon resonances at 29.59 ppm, giving rise to a multiplet rather than the anticipated septet. All other resonances in the spectrum are consistent with the solid-state molecular structure.

With the preparation of these four new diamido-actinide halides **1** and **3**−**5**, as well as the new diamido-thorium dialkyl **9**, combined with the previously reported diamido-uranium halide **2** and diamido-actinide dialkyls **6**−**8**, we sought to examine the behavior of the dialkyl complexes **6**−**9** as precatalysts for intramolecular hydroamination. As a means of including a standard for the reactivity of these dialkyl complexes, complexes **1**−**4** as well as UCl_4 and $ThCl_4$·2DME were also considered. The use of more than one amido R group in this series could provide an insight into the reactivity trends and importance of ligand versus metal choice in these reactions. Chart 1 depicts the new complexes prepared for this study as well as those that have been previously reported (**1**−**9** overall).[65,66]

Chart 1. Diamido−Actinide Complexes 1−9

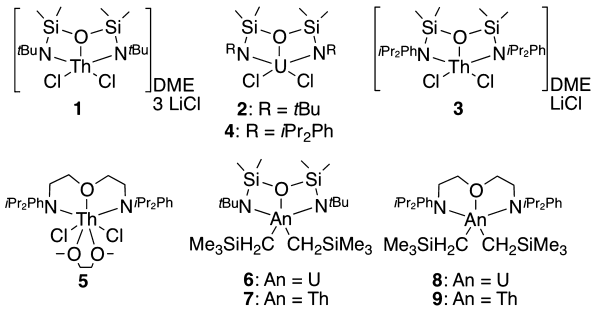

Hydroamination. Initially, complexes **1**−**4** and **6**−**9** were screened for hydroamination activity in the cyclization of **10** (Table 1). We first determined that the parent metal chlorides, UCl_4 and $ThCl_4$·2DME, are inactive for intramolecular hydroamination, even at high temperatures and over prolonged time periods (Table 1, entries 1 and 2). With addition of the diamido silylether ligand, [^{tBu}NON], to the tetrachloride species, high conversions of the aminoalkene **10** are observed

Table 1. Intramolecular Hydroamination of 10 with Complexes 1−4 and 6−9[a]

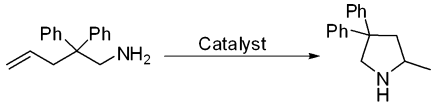

10 **11**

entry	catalyst	catalyst loading (mol %)	temperature (°C)	time (h)	conversion[b] (%)
1	UCl_4	10	110	18	0[c]
2	$ThCl_4$·2DME	10	110	18	0[c]
3	**1**	10	60	4	100[d]
4	**2**	10	60	4	90[d]
5	**3**	10	60	4	0[d]
6	**4**	10	60	4	0[d]
7	**6**	10	23 (room)	2	94
8	**7**	10	23 (room)	2	96
9	**8**	10	23 (room)	1	100
10	**9**	10	23 (room)	<0.25	100
11	**9**	5	23 (room)	<0.25	100
12	**9**	2	23 (room)	<0.25	>90

[a]Reaction conditions: [**10**] = 0.375 M, [1,3,5-trimethoxybenzene] = 0.0625 M in benzene-d_6. [b]Conversion of starting material determined by ^{1}H NMR, relative to 1,3,5-trimethoxybenzene. [c]Reaction in THF-d_8. [d]Reaction in toluene-d_8.

for both dichloride complexes **1** and **2** at 60 °C over 4 h; the Th analogue, **1**, shows higher activity (100% conversion, entry 3) than the U analogue, **2** (90% conversion, entry 4). However, no activity is observed by **1** or **2** at ambient temperature. These results show that use of these ligands allows catalysis at moderate temperatures. While these complexes represent the first actinide dichloride species to be reported as hydroamination precatalysts, close observation of the ^{1}H NMR spectra of the reaction mixtures over the reaction time revealed formation of increasing amounts of the protonated ligand, [^{tBu}NON]H$_2$, indicating that upon coordination to the metal by the aminoalkene substrate, the [^{tBu}NON] ligand is protonated. Interestingly, the related species [^{iPr_2Ph}NON]ThCl_2 (**3**) and [^{iPr_2Ph}]NONUCl_2 (**4**), in which the nitrogen substituent on the ligand is 2,6-di-*iso*-propylphenyl rather than *tert*-butyl, were inactive for the hydroamination of **10** at 60 °C over 4 h (entries 5 and 6). This result is consistent with the reduced basicity of the aromatic substituted amide in comparison to the less basic *tert*-butyl substituted amides, meaning that they are not as easily protonated off by the aminoalkene substrate. In addition, their increased steric bulk is anticipated to affect reactivity. Replacing the chloride ligands of **1** and **2** with dialkyl ligands (complexes **6** and **7**) further increases their activity to the extent that the hydroamination reaction using substrate **10** now proceeds at room temperature, achieving 94% and 96% conversion of starting material, respectively, in 2 h (entries 7 and 8). In this case, it is likely that coordination of the aminoalkene to the metal is accompanied by protonolysis of the −CH_2SiMe_3 ligands to form the metal−amidoalkene species; indeed, the ^{1}H NMR spectra of these reaction mixtures shows no liberation of the ancillary ligand, even at the end of the reactions. Furthermore, the protonolysis of alkyl ligands occurs readily at room temperature, whereas in the case of **1** and **2** no evidence of proligand was observed at room temperature, suggesting elevated temperatures are required for the protonolysis of the [^{tBu}NON] ligand. For this [NON] ligand scaffold, the

dx.doi.org/10.1021/om300410h | *Organometallics* 2012, 31, 6732−6740

differences in activity between U (**6**) and Th (**7**) are negligible and within experimental error.

Moving to the [NCOCN] ethylene bridged diamido ether ligated species, **8** and **9**, the differences in activity between U and Th are more pronounced, with the Th analogue, **9**, being significantly more active than the U analogue, **8**. Repeated experiments with multiple catalyst batches show that while **8** required 1 h in order to generate 100% conversion at room temperature (entry 9), **9** will catalyze the hydroamination of **10** to 100% conversion within 15 min under the same conditions (entry 10). Even at reduced catalyst loadings, as low as 2 mol %, the hydroamination reaction is complete within 15 min using **9** (entries 11 and 12). This actinide-based difference in activity has been reported by others[46] and can be attributed to the greater ionic radius of Th(IV) (1.09 Å) compared to U(IV) (1.05 Å).[74]

It is also useful to compare the [NON] and [NCOCN] backbones in the ligand. However, because the alkylation of **3** and **4** was not successful, the best comparison that can be made is between the activity of **6** and **8** for uranium compounds and that of **7** and **9** for thorium compounds. While **6** requires 2 h to reach 94% conversion of **10**, the reaction reaches completion with **8** within 1 h, indicating higher activity for the [NCOCN] ligand. This trend of higher activity for the [NCOCN] ligand is also evident, and in fact more dramatic, in the case of thorium: **7** requires 2 h to reach 95% conversion of **10** at room temperature, while **9** catalyzes the reaction in just 15 min. These results suggest that the [NCOCN] ligands promote greater reactivity than the [NON] ligands despite the differences in nitrogen substituents. One would expect that greater steric bulk around the metal would slow the rate of catalysis; here, the complexes with ligands containing bulkier nitrogen substituents (**8** and **9**) are more active than those with less bulky substituents (**6** and **7**). However, the enhanced reactivity of ligand sets featuring the bulky 2,6-di-*iso*-propylphenyl substituent has been observed previously in early transition metal catalyzed hydroamination.[75] The thermal stability of this family of complexes in solution has been confirmed by variable temperature NMR spectroscopy across the range of temperatures[65,66] used in this investigation, and more specifically the dialkyl derivatives **6**–**9** have been heated to 100 °C and cooled with no changes in the ^{1}H NMR spectra. Furthermore, no evidence of ancillary ligand protonation or fragmentation over the course of the hydroamination reactions has been observed, so these differences in reactivity can be attributed to the differing ligand structures.

Having identified **9** as the most active hydroamination precatalyst in the screening reaction above, we went on to explore the scope of reactivity with this species. For a broad comparison of the differences in activity imposed by the ligand structure, we chose **7** and, in addition, selected **8** in order to be able to directly compare differences between U and Th when using the same ligand. A number of terminal aminoalkene substrates were used to test complexes **7**–**9**; the results are presented in Table 2.

All three complexes, **7**, **8**, and **9**, are able to cyclize **10** efficiently at room temperature, and these results were used as a benchmark (Table 2, entries 1–3). First, we wanted to compare the complexes' ability to form different sized rings and selected aminoalkene substrates **10**, **12**, and **22**, which would form 5-, 6-, and 7-membered rings, respectively, in order to do this. In comparison to the room temperature reactivity observed for **10**, when 10 mol % of **9** was reacted with **12** at room temperature,

Table 2. Intramolecular Hydroamination of Various Aminoalkenes with Diamido–Actinide Dialkyl Catalysts 7,8, and 9.[a]

	substrate	product	cat	T °C	time h	conv %[b]
1	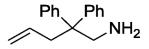	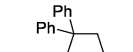	**7**	23	2	96
2			**8**	23	1	100
3	**10**	**11**	**9**	23	<0.25	100
4	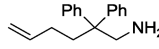	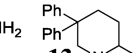	**7**	60	5.5	100
5			**8**	60	2	100
6	**12**	**13**	**9**	60	2	95
7	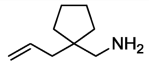	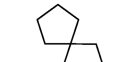	**7**	60	2	96
8			**9**	60	2	94
	14	**15**				
9	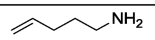	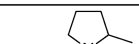	**7**	110	72	13
10	**16**	**17**	**8**	110	72	12
11			**9**	110	72	7
12	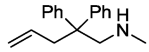	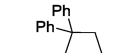	**7**	80	19.5	81
13			**8**	60	2	78
14	**18**	**19**	**9**	80	16	92
15	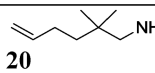	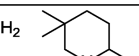	**8**	80	18	94
	20	**21**				

[a]Reaction conditions: [aminoalkene] = 0.375 M, [**7**–**9**] = 0.0375 M [1,3,5-trimethoxybenzene] = 0.0625 M in benzene-d_6. [b]Conversion of starting material, determined by ^{1}H NMR, relative to 1,3,5-trimethoxybenzene.

just 3% conversion of starting material was observed after 2 h. Thus the reaction mixture was heated at 60 °C for 2 h, whereupon 95% conversion of **12** was observed (entry 6). Since **7** is less reactive than **9**, its reaction with **12** was monitored at 60 °C rather than room temperature. The lower reactivity of **7** is confirmed as only 42% conversion of the aminoalkene was observed after 2 h, a further 3.5 h was required for 100% conversion to occur (entry 4). Surprisingly, **8** showed higher room temperature activity than **9** in this reaction, giving 15% conversion of **12** over 2 h at room temperature. Here, 100% conversion to **13** was observed at 60 °C over 2 h (entry 5). This behavior, where Th analogues of a given species are more efficient than U in the formation of 5-membered rings, but U is more active than Th in the formation of 6-membered rings has been observed previously in Cp-based actinide systems,[46] where this observation was attributed to the finely tuned steric requirements for intramolecular hydromination.

Azepane formation was challenging for both **8** and **9**, more so for **9** (Scheme 2). In an initial reaction, no appreciable conversion of **22** to **23** was observed either at room temperature or 60 °C over 2 h with either catalyst. Indeed, even heating to 80 °C for 16 h gave <5% conversion of starting material. Only when the reaction mixture was heated at 110 °C was some reactivity observed with **9**: 11% over 24 h. The

Scheme 2. Azepane Formation with 8 and 9

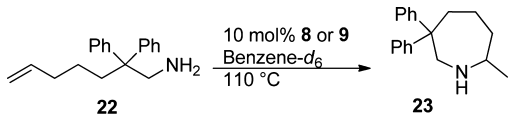

22 **23**

8 18 h 33%
9 72 h 28%

dx.doi.org/10.1021/om300410h | *Organometallics* 2012, 31, 6732–6740

reaction was repeated, heating immediately at 110 °C, and 28% conversion of **22** was observed over 72 h. Again, **8** is considerably more active than **9** for this substrate, reaching 33% conversion in 18 h, although high temperatures are still required for this transformation. Because of the previously observed lower activity of **7** compared to **9**, **7** was not tested as a precatalyst for hydroamination of this substrate.

The effect of *gem*-disubstitution in the aminoalkenes was investigated by comparison of the activity of **7** and **9** in the cyclization of **10**, **14**, and **16**, Table 2. Conversion of unsubstituted **16** to **17** was extremely sluggish for all three complexes, reaching only 7−13% conversion even at 110 °C over 72 h (entries 9−11). No reactivity was observed for these reactions at room temperature, 60 or 80 °C. This observation is in agreement with the Thorpe−Ingold effect. Having been efficient in 6-membered ring formation, **8** was used to cyclize **20**, with less bulky *gem*-dimethyl groups rather than *gem*-diphenyl groups. While 2 h at 60 °C yields 100% conversion of **12** to **13** (entry 5), under the same conditions, **20** is only 23% converted to **21**; 18 h at 80 °C is needed for 94% conversion (entry 15). These results are also in agreement with the Thorpe−Ingold effect and confirm that reduction of steric bulk in *gem*-substituents makes cyclization challenging. Cyclization of **14** to the bicyclic product **15** by **7** or **9** also proceeded at room temperature, although the reactions were much slower than for their diphenyl substituted counterpart, reaching 41% and 52% conversion in 4 h, respectively. At 60 °C, these reactions were largely complete within 2 h (entries 7 and 8).

We were interested in determining whether any of the complexes are able to catalyze hydroamination with a secondary amine, as this might provide some insight into the reaction mechanism. If an imido mechanism is in operation,[43] hydroamination of secondary amines would not be expected to occur; cyclization of **18** to **19** would indicate a σ-bond insertion mechanism. Proposals for the mechanism of hydroamination by actinide complexes include both imido[43,44] and σ-bond insertion mechanisms.[47] Interestingly, it has been suggested that a ferrocene−diamide uranium precatalyst was capable of catalyzing hydroamination by both a σ-bond insertion and an imido mechanism.[48] In our case, when the reaction of **18** with 10 mol % of **9** was carried out, a negligible amount of conversion (<2%) was observed after 2 h at room temperature. Heating the reaction mixture to 60 °C for 2 h gave 18% conversion, and 92% conversion was only achieved after 16 h at 80 °C (entry 14). We can compare the activity of **9** in the cyclization of **10** and **18** (entries 3 and 14), where the only difference between the substrates is an *N*-methyl substituent. Where as **10** is cyclized with ease in very little time at room temperature, **18** requires elevated temperatures for hydroamination to occur. Similar observations have been reported by others.[47,48] In contrast to the two thorium complexes, the uranium complex, **8**, showed room temperature activity in the cyclization of **18**, reaching 12% conversion after 1 h at room temperature. Furthermore, an increase in reaction temperature to 60 °C gave 78% conversion in 2 h, showing **8** to be more proficient in secondary amine hydroamination than both **7** and **9** at lower temperature (entry 13). This switch in activity between uranium and thorium has also been previously observed by others,[47] although the origins of this interesting behavior are unclear.

CONCLUSIONS

Diamido-ether thorium(IV) and uranium(IV) complexes **1**−**5** were prepared from the corresponding tetrachloride precursors. The use of $ThCl_4$·2DME results in either "ate" complex formation (as in the case of **1** and **3**) or retention of a DME molecule in the final product (as in **5**). Despite the formation of "ate" complexes, these dihalides can be cleanly alkylated to give the corresponding base- and salt-free dialkyls **7** and **9**. Diamido-actinide dihalides **1**−**4** and diamido-actinide dialkyls **6**−**9** were tested for activity in intramolecular hydroamination. Complexes **1** and **2** were found to facilitate the cyclization of **10** at 60 °C over the course of 4 h, although product formation was concomitant with complex decomposition. Complexes **3** and **4** did not show any activity for the same reaction under the same conditions. This indicates that the chloride ligands are not active in hydroamination. Complexes **6**−**9** were also tested for activity with **10** and show full conversion at room temperature in 2 h or less (in the case of **9**, the reaction occurs in less than 15 min) with no catalyst decomposition. The substrate scope of complexes **7**−**9** was also explored in an effort to better understand the reactivity of these compounds. While all three facilitated the cyclization of **10** quickly at room temperature, **8** proved to be more active for the cyclization of 6- and 7-membered rings, **12** (100% in 2 h, at 60 °C) and **22** (33% in 18 h, at 110 °C), respectively. Complex **8** also showed higher activity for the cyclization of a secondary amine, **18** (78% in 2 h, at 60 °C). However, all three catalysts (**7**−**9**) showed decreasing activity with decreasing steric bulk of the *gem*-substituents of substrates **14** and **16**.

A direct comparison of the hydroamination activity of complexes **6**−**8** with other reported actinide complexes is difficult, largely due to differing reaction conditions. More broadly, although the activities for the hydroamination of primary amine substrates with bulky *gem*-substitutents for **6**−**8** are comparable to Cp^*AnMe_2 systems, a limitation of the complexes reported here lies in the loss of activity for amines without gem-substitution. These results show that Th is more active than U typically, while the less rigid fused 5-membered metallacycles of [^{iPr_2Ph}NCOCN] generate the more catalytically active complexes. Consistent with previous reports, 2,6-di-*iso*-propylphenyl is a preferred N-substituent, resulting in a thermally robust Th and U complex, where U does display enhanced reactivity with select substrates.

EXPERIMENTAL SECTION

General Procedures. All techniques and procedures were carried out under a nitrogen atmosphere either with an Mbraun Labmaster 130 glovebox or using standard Schlenk and vacuum-line techniques. All glassware was dried overnight at 160 °C prior to use. Toluene, tetrahydrofuran (THF), dimethoxyethane (DME), and diethyl ether were distilled from a sodium/benzophenone solution under nitrogen. Hexanes were distilled from a sodium solution under nitrogen. Deuterated solvents were distilled from a sodium/benzophenone solution and freeze−pump−thawed three times before use. UCl_4,[76] $ThCl_4$·2DME,[62] $[(CH_3)_3CNH(Si(CH_3)_2)]_2O$,[77,78] $[2,6\text{-}^iPr_2PhNH(Si(CH_3)_2)]_2O$,[79] $[2,6\text{-}^iPr_2PhNH(CH_2CH_2)]_2O$,[80] $[^{tBu}NON]UCl_2\}_2$ (**2**),[65] $[^{tBu}NON]U(CH_2SiMe_3)_2$ (**6**),[65] $[^{tBu}NON]Th(CH_2SiMe_3)_2$ (**7**),[65] $[^{iPr2Ph}NCOCN]U(CH_2SiMe_3)_2$ (**8**),[66] 2,2-diphenyl-1-amino-4-pentene (**10**),[81] 2,2-diphenyl-1-amino-5-hexene (**12**),[81] 2,2-diphenyl-1-amino-6-heptene (**22**),[82] (1-allylcyclopentyl)methanamine (**14**),[83] 1-amino-4-pentene (**16**),[82] *N*-methyl-2,2-diphenyl-1-amino-4-pentene (**18**),[46] and 2,2-dimethyl-1-amino-5-hexene (**20**)[84] were prepared in accordance with published literature procedures. Pentane was removed *in vacuo* from $LiCH_2Si(CH_3)_3$ (1.0 M, Aldrich) prior to use. All other

dx.doi.org/10.1021/om300410h | *Organometallics* 2012, 31, 6732−6740

reagents were purchased from commercial sources and used without further purification. NMR spectra were recorded at 294 K, unless otherwise stated, on either a 400 MHz Bruker Avance III spectrometer, a 500 MHz Bruker Avance III spectrometer, or a 600 MHz Bruker Avance II spectrometer with a 5 mm QNP cryoprobe. All ^{1}H NMR shifts are reported in ppm relative to the impurity of internal solvent: specifically, benzene-d_6 at δ 7.15 or toluene-d_8 at δ 2.06. Elemental analyses (C, H, N) were performed at Simon Fraser University by Farzad Haftbaradaran by employing a Carlo Erba EA 1110 CHN elemental analyzer.

[$^{t\mathrm{Bu}}$NON]ThCl$_5$Li$_3$·DME (1). [$^{t\mathrm{Bu}}$NON]H$_2$ (0.449 g, 1.63 mmol) was dissolved in diethyl ether, and 2 equiv of ^{n}BuLi (1.30 mL, 3.25 mmol) were added dropwise at 0 °C, resulting in a cloudy white solution. The reaction was warmed to room temperature and transferred via syringe to a cold (−78 °C) solution of ThCl$_4$·2DME (0.901 g, 1.63 mmol) in diethyl ether. Upon warming to room temperature, the reaction was cloudy and beige in color, and stirring was continued at room temperature for 3 days. Excess solvent was removed *in vacuo* to yield a beige powder, which was extracted with toluene and filtered through a Celite-padded medium-porosity glass frit. Excess toluene was removed *in vacuo* to yield a beige powder of [$^{t\mathrm{Bu}}$NON]ThCl$_5$Li$_3$·DME (**1**) (0.80 g, 62%). Anal. Calcd for $C_{16}H_{40}N_2O_3Si_2Cl_5Li_3Th$: C, 24.18; H, 5.07; N, 3.52. Found: C, 24.37; H, 5.06; N, 3.17. ^{1}H NMR (THF-d_8): δ 0.89 (s, 6H, Si(CH_3)$_2$), 1.31 (s, 6H, Si(CH_3)$_2$), 1.33 (s, 18H, C(CH_3)$_3$), 3.27 (s, 6H, O-CH_3), 3.43 (s, 4H, O-CH_2). ^{13}C{^{1}H} NMR (THF-d_8): δ 5.57 (Si(CH$_3$)$_2$), 27.11 (C(CH$_3$)$_2$), 34.57 (C(CH$_3$), 35.15 (Si(CH$_3$)$_2$), 52.34 (O-CH$_3$), 72.91 (O-CH$_2$).

[$^{i\mathrm{Pr}_2\mathrm{Ph}}$NON]ThCl$_3$Li·DME (3). [$^{i\mathrm{Pr}_2\mathrm{Ph}}$NON]H$_2$ (0.131 g, 0.27 mmol) was dissolved in diethyl ether, and 2 equiv of ^{n}BuLi (0.22 mL, 0.54 mmol) was added dropwise at 0 °C, resulting in a clear bright-yellow solution. The reaction was warmed to room temperature and transferred via syringe to a cold (−78 °C) solution of ThCl$_4$·2DME (0.150 g, 0.27 mmol) in diethyl ether. Upon warming to room temperature, the reaction was cloudy and bright-orange in color; stirring was continued at room temperature for 18 h. Excess solvent was removed *in vacuo* to yield an orange oil. This solid was extracted with toluene and filtered through a Celite-padded medium-porosity glass frit. Excess toluene was removed *in vacuo* to yield an orange−yellow powder of [$^{i\mathrm{Pr}_2\mathrm{Ph}}$NON]ThCl$_3$Li·DME (**3**) (0.121 g, 48%). Anal. Calcd. for $C_{32}H_{56}N_2O_3Si_2Cl_3LiTh$: C, 41.85; H, 6.15; N, 3.05. Found: C, 41.82; H, 6.29; N, 2.97. ^{1}H NMR (toluene-d_8): δ 0.26 (s, 12H, Si(CH_3)$_2$), 1.14 (d, 6H, CH(CH_3)$_2$), 1.22 (d, 6H, CH(CH_3)$_2$), 1.27 (d, 6H, CH(CH_3)$_2$), 1.45 (d, 6H, CH(CH_3)$_2$), 2.93 (br s, 4H, O-CH_2 DME), 3.23 (br s, 6H, O-CH_3 DME), 3.58 (sept, 1H, CH(CH$_3$)$_2$, 4.20 (sept, 1H, CH(CH$_3$)$_2$), 6.88−7.14 (m, 6H, Ar-H). ^{13}C{^{1}H} NMR (toluene-d_8): δ 1.77 (Si(CH$_3$)$_2$), 4.24 (SiCH$_3$)$_2$), 22.93 (CH(CH$_3$)$_2$), 24.29 (CH(CH$_3$)$_2$), 27.02 (CH(CH$_3$)$_2$), 27.42 (CH(CH$_3$)$_2$), 60.16 (O-CH$_3$, DME), 70.95 (O-CH$_2$, DME), 123.78 (Ar-*para*), 124.90 (Ar-*para*), 128.62 (Ar-*meta*), 129.54 (Ar-*meta*), 132.64 (*C*-CH(CH$_3$)$_2$), 144.93 (N-Ar-*C*), 145.07 (N−Ar-*C*).

{[$^{i\mathrm{Pr}_2\mathrm{Ph}}$NON]UCl$_2$}$_2$ (4). [$^{i\mathrm{Pr}_2\mathrm{Ph}}$NON]H$_2$ (0.316 g, 0.32 mmol) was dissolved in diethyl ether, and 2 equiv of ^{n}BuLi (0.25 mL, 0.63 mmol) was added dropwise at 0 °C, resulting in a clear bright-yellow solution. The reaction was warmed to room temperature and transferred via syringe to a cold (−78 °C) solution of UCl$_4$ (0.120 g, 0.32 mmol) in diethyl ether. Upon warming to room temperature, the reaction became cloudy and orange−brown in color; stirring was continued at room temperature for 18 h. Excess solvent was removed *in vacuo* to yield a brown solid. This solid was extracted with toluene and filtered through a Celite-padded medium-porosity glass frit. Excess toluene was removed *in vacuo* to yield a brown−orange powder of {[$^{i\mathrm{Pr}_2\mathrm{Ph}}$NON]UCl$_2$}$_2$ (**4**) (0.235 g, 94%). Crystals suitable for X-ray diffraction were grown by slow evaporation of a toluene solution. Anal. Calcd for $C_{63}H_{100}N_4O_2Si_4Cl_4U_2$: C, 45.16; H, 6.02; N, 3.34. Found: C, 45.51; H, 6.35; N, 3.53. ^{1}H NMR (toluene-d_8, 298 K) δ −9.61 (v br s), −4.21 (s), −2.84 (s), −0.41 (s), 5.33 (s), 6.08 (s), 6.46 (v br s), 7.73 (v br s), 9.25 (s), 9.45 (s), 10.76, (s), 11.12 (v br s), 15.49 (v br s); (toluene-d_8, 338 K) δ −8.49 (vv br s), −3.62 (s), −2.40 (s), −0.14 (s), 4.91 (s), 5.54 (s), 6.68 (s), 6.81 (s), 9.08 (s), 9.22 (s), 9.79 (v br s), 10.39 (s), 14.27 (v br s); (toluene-d_8, 358 K) δ −8.67 (v br s), −7.99 (v br s), −3.35 (s), −2.20 (s), 0.00 (s), 2.95 (br s), 4.72 (s), 5.30 (s), 6.38 (br s), 9.01 (s), 9.12 (s), 9.22 (br s), 10,23 (s), 13.76 (v br s); (toluene-d_8, 298 K after heating) δ −9.58 (v br s), −4.22 (s), −2.85 (s), −0.42 (s), 5.33 (s), 6.07 (s), 7.72 (v br s), 9.24 (s), 9.45 (s), 10.75 (s), 10.98 (v br s), 15.46 (v br s).

[$^{i\mathrm{Pr}_2\mathrm{Ph}}$NCOCN]ThCl$_2$·DME (5). [$^{i\mathrm{Pr}_2\mathrm{Ph}}$NCOCN]H$_2$ (0.521 g, 1.23 mmol) was dissolved in diethyl ether, and 2 equiv of ^{n}BuLi (0.98 mL, 2.46 mmol) were added dropwise at 0 °C, resulting in a cloudy yellow solution. The reaction was warmed to room temperature and transferred via syringe to a cold (−78 °C) solution of ThCl$_4$·2DME (0.679 g, 1.23 mmol) in diethyl ether. Upon warming to room temperature, the reaction became cloudy orange in color, and stirring was continued at room temperature for 3 days. Excess solvent was removed *in vacuo* to yield an orange solid. This solid was extracted with toluene and filtered through a Celite-padded medium-porosity glass frit. Excess toluene was removed *in vacuo* to yield an orange powder of [$^{i\mathrm{Pr}_2\mathrm{Ph}}$NCOCN]ThCl$_2$·DME (**5**) (0.97 g, 97%). Crystals suitable for X-ray diffraction were grown by slow evaporation of a DME−toluene solution. Anal. Calcd for $C_{32}H_{52}N_2O_3Cl_2Th$: C, 47.12; H, 6.43; N, 3.43. Found: C, 47.37; H, 6.58; N, 3.31. ^{1}H NMR (THF-d_8): δ 1.06 (d, 12H, CH(CH_3)$_2$), 1.32 (d, 12H, CH(CH_3)$_2$), 3.27 (s, 6H, O-CH_3 DME), 3.43 (s, 4H, O-CH_2 DME), 3.76 (t, 4H, N-CH_2), 4.19 (m, 4H, CH(CH$_3$)$_2$), 4.43 (t, 4H, O-CH_2), 6.90 (t, 2H, N-Ar-*para*), 7.05 (d, 4H, N-Ar-*meta*). ^{13}C{^{1}H} NMR (THF-d_8): δ 24.21 (CH(CH$_3$)$_2$), 24.50 (CH(CH$_3$)$_2$), 28.39 (CH(CH$_3$)$_2$), 35.21 (N-CH$_2$), 52.65 (N-CH$_2$), 59.07 (O-CH$_3$ DME), 68.76 (O-CH$_2$), 72.91 (O-CH$_2$ DME), 124.21 (Ar-CH), 124.75 (Ar-CH), 148.13 (Ar-*C*), 149.79 (Ar-*C*).

[$^{t\mathrm{Bu}}$NON]Th(CH$_2$SiMe$_3$)$_2$ (7). **1** (0.452 g, 0.73 mmol) was dissolved in toluene, and 2 equiv of LiCH$_2$SiMe$_3$ (0.138 g, 1.46 mmol) were added. Upon addition, the reaction turned bright-yellow in color. Stirring was continued at room temperature for 18 h. The reaction was filtered through a Celite-padded medium-porosity glass frit using hexanes as the solvent, resulting in a clear yellow solution. Excess hexanes was removed *in vacuo* to yield a yellow oil of [$^{t\mathrm{Bu}}$NON]Th(CH$_2$SiMe$_3$)$_2$ (**7**) (0.322 g, 83%). The ^{1}H, ^{13}C{^{1}H} NMR spectra, and elemental analysis are consistent with the previously published synthesis of **7**.[65]

[$^{i\mathrm{Pr}_2\mathrm{Ph}}$NCOCN]Th(CH$_2$SiMe$_3$)$_2$ (9). [$^{i\mathrm{Pr}_2\mathrm{Ph}}$NCOCN]ThCl$_2$·DME (0.197 g, 0.241 mmol) was dissolved in toluene, and 2 equiv of LiCH$_2$SiMe$_3$ (0.045 g, 0.482 mmol) were added. Upon addition, the reaction turned bright-orange in color. Stirring was continued at room temperature for 18 h. The reaction was filtered through a Celite-padded medium-porosity glass frit using toluene as the solvent, resulting in a clear-orange solution. Excess toluene was removed *in vacuo* to yield a pale-orange powder of [$^{i\mathrm{Pr}_2\mathrm{Ph}}$NCOCN]Th(CH$_2$SiMe$_3$)$_2$ (**9**) (0.184 g, 92%). Crystals suitable for X-ray diffraction were grown by slow evaporation of a hexanes solution. Anal. Calcd for $C_{36}H_{64}N_2OSi_2Th$: C, 52.15; H, 7.78; N, 3.38. Found: C, 51.95; H, 7.61; H, 2.99. ^{1}H NMR (benzene-d_6): δ −0.37 (s, 4H, CH_2SiMe$_3$), 0.11 (s, 18H, CH$_2$Si(CH_3)$_3$), 1.22 (d, 12H, CH(CH_3)$_2$), 1.49 (d, 12H, CH(CH_3)$_2$), 3.48 (t, 4H, O-CH_2), 3.53 (t, 4H, N-CH_2), 3.64 (m, 4H, CH(CH$_3$)$_2$), 6.85−7.02 (m, 6H, Ar-H). ^{13}C{^{1}H} NMR (benzene-d_6): δ 4.15 (CH$_2$Si(CH$_3$)$_3$), 24.77 (CH(CH$_3$)$_2$), 27.35 (CH(CH$_3$)$_2$), 29.59 (CH(CH$_3$)$_2$), 58.38 (N-CH$_2$), 76.36 (O-CH$_2$), 90.73 (CH$_2$SiMe$_3$), 125.02 (Ar-*ortho*), 126.85 (N-Ar-*para*), 143.26 (N-Ar-*ispo*), 137.58 (N-Ar-*meta*).

Typical Procedure for Hydroamination. Complex **6** (0.026 g, 0.0375 mmol, 10 mol %), 1,3,5-trimethoxybenzene (0.011 g, 0.0625 mmol), and 2,2-diphenyl-1-amino-4-pentene (0.089 g, 0.375 mmol) were weighed into separate vials, dissolved, and combined in approximately 0.5 g of deuterated benzene (or deuterated toluene for **1**−**4**) in a J-Young sealable NMR tube. The ^{1}H NMR spectrum was obtained within 15 min to monitor conversion. By comparison of the integration values for the proton signals of the 1,3,5-trimethoxybenzene (δ 6.25 and 3.32 for aryl-H and −O(CH_3) protons, respectively) to the newly formed CH(CH$_3$) signal (2.47 ppm) in the ^{1}H NMR spectrum, the NMR the yield was obtained.

dx.doi.org/10.1021/om300410h | *Organometallics* 2012, 31, 6732−6740

Table 3. Summary of Crystallographic Data

	4	5	9
formula	$C_{28}H_{46}Cl_2N_2OSi_2U$	$C_{32}H_{52}Cl_2N_2O_3Th$	$C_{36}H_{64}N_2OSi_2Th$
M_w	791.79	815.72	829.13
cryst dimensions/mm^3	0.12 × 0.16 × 0.16	0.18 × 0.22 × 0.30	0.13 × 0.25 × 0.70
crystal system	monoclinic	orthorhombic	orthorhombic
space group	$P2(1)/n$	$P2(1)$	$Pbca$
T/K	150	293	293
a/Å	14.0202(7)	8.0499(10)	11.5075(4)
b/Å	12.8943(7)	16.871(2)	20.0888(6)
c/Å	20.3938(10)	26.702(3)	35.4127(12)
α/deg	90	90	90
β/deg	102.2880(10)	90	90
γ/deg	90	90	90
V/Å^3	3602.3(3)	3626.4(8)	8186.4(5)
Z	4	4	8
D_c/g cm^{-3}	1.460	1.494	1.345
μ/cm^{-1}	4.741	4.290	3.728
R ($I > 2.5\sigma(I)$)[a]	0.0498	0.0237	0.0710
R_w ($I > 2.5\sigma(I)$)[a]	0.0783	0.0233	0.0441
GOF	2.3686	0.9903	1.5847

[a]The function minimized was $\sum w(|F_o| - |F_c|)^2$, where $w^{-1} = [\sigma^2(F_o) + (nF_o)^2]$ with n = 0.02 for **4**, 0.02 for **5**, and 0.04 for **9**. $R = \sum||F_o| - |F_c||/\sum|F_o|$; $R_w = [\sum w(|F_o| - |F_c|)^2/\sum w|F_o|^2]^{1/2}$.

X-ray Crystallography. Crystallographic data for all structures are collected in Table 3. For **5** and **9**, suitable crystals were loaded into 0.5 mm glass-walled capillaries suitable for X-ray diffraction and flame sealed under nitrogen. For **4**, the crystals were coated in paratone oil, mounted on a MiTeGen Micro Mount, and transferred to the cold stream (150 K) of the X-ray diffractometer. Crystal descriptions for each compound are as follows: **4** is a green rectangular block with dimensions of 0.12 × 0.16 × 0.16 mm^3; **5** is a yellow rectangular block with dimensions of 0.18 × 0.22 × 0.30 mm^3; **9** is a white rectangular block with dimensions of 0.7 × 0.25 × 0.13 mm^3. All data was collected on a Bruker Smart instrument equipped with an APEX II CCD area detector fixed at a distance of 6.0 cm from the crystal (for **5** the distance was fixed at 8.0 cm) and a Mo Kα fine focus sealed tube (λ = 0.71073 nm) operated at 1.5 kW (50 kV, 30 mA) and filtered with a graphite monochromator. Temperature was regulated using an Oxford Cryosystems Cryostream; **4** was collected at 150 K, and **5** and **9** were collected at 293 K. Data reduction and absorption correction details can be found in the crystal information file (Supporting Information).

The structures were solved using direct methods (SIR 92) and refined by least-squares procedures using CRYSTALS.[85] Hydrogen atoms on carbon atoms were included at geometrically idealized positions (C−H bond distance 0.95) and were not refined. The isotropic thermal parameters of the hydrogen atoms were fixed at 1.2 times that of the preceding carbon atom. The plots for the crystal structures were generated using ORTEP-3 for windows (v. 2.00)[86] and rendered using POV-Ray (v. 3.6.1).[87] Thermal ellipsoids are shown at the 30% probability level.

For **4** and **5**, coordinates and anisotropic displacement parameters for all non-hydrogen atoms were refined. For **9**, coordinates and anisotropic displacement parameters for all non-hydrogen atoms were refined, with the exception of one $CH_2Si(CH_3)_3$ group, which was found to be rotationally disordered and was treated accordingly. The Flack enantiopole parameter (0.008(5)) was included in the final refinement cycles of **5**.

■ ASSOCIATED CONTENT

Supporting Information

Complete crystallographic data in CIF format for all three reported crystal structures. This material is available free of charge via the Internet at http://pubs.acs.org.

■ AUTHOR INFORMATION

Corresponding Author

*For D.B.L.: phone, 778-782-4887; fax, 778-782-3765; E-mail, dleznoff@sfu.ca. For L.L.S.: phone, 604-822-9264; fax, 604-822-2847; E-mail, schafer@chem.ubc.ca.

Notes

The authors declare no competing financial interest.

■ ACKNOWLEDGMENTS

This work was supported by NSERC of Canada and Canada Research Chair in Catalyst Development to L.L.S. C.E.H. is grateful to NSERC for a PGS-D and SFU for a President's Research Stipend and Graduate Fellowships.

■ REFERENCES

(1) Hultzsch, K. C. *Org. Biomol. Chem.* **2005**, *3*, 1819.
(2) Müller, T. E.; Beller, M. *Chem. Rev.* **1998**, *98*, 675.
(3) Müller, T. E.; Hultzsch, K. C.; Yus, M.; Foubelo, F.; Tada, M. *Chem. Rev.* **2008**, *108*, 3795.
(4) Severin, R.; Doye, S. *Chem. Soc. Rev.* **2007**, *36*, 1407.
(5) Hultzsch, K. C. *Adv. Synth. Catal.* **2005**, *347*, 367.
(6) Ackermann, L.; Bergman, R. G.; Loy, R. N. *J. Am. Chem. Soc.* **2003**, *125*, 11956.
(7) Gott, A. L.; Clarke, A. J.; Clarkson, G. J.; Scott, P. *Organometallics* **2007**, *26*, 1729.
(8) Kim, H.; Lee, P. H.; Livinghouse, T. *Chem. Commun.* **2005**, 5205.
(9) Kubiak, R.; Prochnow, I.; Doye, S. *Angew. Chem., Int. Ed.* **2010**, *49*, 2626.
(10) Lee, A. V.; Schafer, L. L. *Eur. J. Inorg. Chem.* **2007**, 2243.
(11) Leitch, D. C.; Payne, P. R.; Dunbar, C. R.; Schafer, L. L. *J. Am. Chem. Soc.* **2009**, *131*, 18246.
(12) Li, C. Y.; Thomson, R. K.; Gillon, B.; Patrick, B. O.; Schafer, L. L. *Chem. Commun.* **2003**, 2462.
(13) Majumder, S.; Odom, A. L. *Organometallics* **2008**, *27*, 1174.
(14) Manna, K.; Xu, S.; Sadow, A. D. *Angew. Chem., Int. Ed.* **2011**, *50*, 1865.
(15) Müller, C.; Saak, W.; Doye, S. *Eur. J. Org. Chem.* **2008**, 2731.
(16) Odom, A. L. *Dalton Trans.* **2005**, 225.
(17) Wang, X.; Chen, Z.; Sun, X.-L.; Tang, Y.; Xie, Z. *Org. Lett.* **2011**, *13*, 4758.

(18) Watson, D. A.; Chiu, M.; Bergman, R. G. *Organometallics* **2006**, *25*, 4731.
(19) Wood, M. C.; Leitch, D. C.; Yeung, C. S.; Kozak, J. A.; Schafer, L. L. *Angew. Chem., Int. Ed.* **2007**, *46*, 354.
(20) Komeyama, K.; Morimoto, T.; Takaki, K. *Angew. Chem., Int. Ed.* **2006**, *45*, 2938.
(21) Ohmiya, H.; Moriya, T.; Sawamura, M. *Org. Lett.* **2009**, *11*, 2145.
(22) Hesp, K. D.; Stradiotto, M. *Org. Lett.* **2009**, *11*, 1449.
(23) Liu, Z.; Hartwig, J. F. *J. Am. Chem. Soc.* **2008**, *130*, 1570.
(24) Bender, C. F.; Widenhoefer, R. A. *J. Am. Chem. Soc.* **2005**, *127*, 1070.
(25) Cochran, B. M.; Michael, F. E. *J. Am. Chem. Soc.* **2008**, *130*, 2786.
(26) Cochran, B. M.; Michael, F. E. *Org. Lett.* **2008**, *10*, 329.
(27) Han, X. Q.; Widenhoefer, R. A. *Angew. Chem., Int. Ed.* **2006**, *45*, 1747.
(28) Liu, X.-Y.; Li, C.-H.; Che, C.-M. *Org. Lett.* **2006**, *8*, 2707.
(29) Zhang, J. L.; Yang, C. G.; He, C. *J. Am. Chem. Soc.* **2006**, *128*, 1798.
(30) Alonso, F.; Beletskaya, I. P.; Yus, M. *Chem. Rev.* **2004**, *104*, 3079.
(31) Gottfriedsen, J.; Edelmann, F. T. *Coord. Chem. Rev.* **2006**, *250*, 2347.
(32) Edelmann, F. T. *Coord. Chem. Rev.* **2006**, *250*, 2511.
(33) Hong, S.; Marks, T. J. *Acc. Chem. Res.* **2004**, *37*, 673.
(34) O'Shaughnessy, P. N.; Knight, P. D.; Morton, C.; Gillespie, K. M.; Scott, P. *Chem. Commun.* **2003**, 1770.
(35) Kim, Y. K.; Livinghouse, T.; Horino, Y. *J. Am. Chem. Soc.* **2003**, *125*, 9560.
(36) Kim, J. Y.; Livinghouse, T. *Org. Lett.* **2005**, *7*, 1737.
(37) Panda, T. K.; Hrib, C. G.; Jones, P. G.; Jenter, J.; Roesky, P. W.; Tamm, M. *Eur. J. Inorg. Chem.* **2008**, 4270.
(38) Rastätter, M.; Zulys, A.; Roesky, P. W. *Chem.—Eur. J.* **2007**, *13*, 3606.
(39) Rastätter, M.; Zulys, A.; Roesky, P. W. *Chem. Commun.* **2006**, 874.
(40) Wang, Q.; Xiang, L.; Song, H.; Zi, G. *Inorg. Chem.* **2008**, *47*, 4319.
(41) Haskel, A.; Straub, T.; Eisen, M. S. *Organometallics* **1996**, *15*, 3773.
(42) Eisen, M. S.; Straub, T.; Haskel, A. *J. Alloys Compd.* **1998**, *271*, 116.
(43) Straub, T.; Haskel, A.; Neyroud, T. G.; Kapon, M.; Botoshansky, M.; Eisen, M. S. *Organometallics* **2001**, *20*, 5017.
(44) Wang, J. X.; Dash, A. K.; Kapon, M.; Berthet, J.-C.; Ephritikhine, M.; Eisen, M. S. *Chem.—Eur. J.* **2002**, *8*, 5384.
(45) Stubbert, B. D.; Stern, C. L.; Marks, T. J. *Organometallics* **2003**, *22*, 4836.
(46) Stubbert, B. D.; Marks, T. J. *J. Am. Chem. Soc.* **2007**, *129*, 4253.
(47) Stubbert, B. D.; Marks, T. J. *J. Am. Chem. Soc.* **2007**, *129*, 6149.
(48) Broderick, E. M.; Gutzwiller, N. P.; Diaconescu, P. L. *Organometallics* **2010**, *29*, 3242.
(49) Barnea, E.; Eisen, M. S. *Coord. Chem. Rev.* **2006**, *250*, 855.
(50) Andrea, T.; Eisen, M. S. *Chem. Soc. Rev.* **2008**, *37*, 550.
(51) Katz, J. J.; Seaborg, G. T.; Morss, L. R. *The Chemistry of the Actinide Elements*; Chapman and Hall: New York, 1986.
(52) Edelmann, F. T. *Angew. Chem., Int. Ed.* **1995**, *34*, 2466.
(53) Edelmann, F. T.; Freckmann, D. M. M.; Schumann, H. *Chem. Rev.* **2002**, *102*, 1851.
(54) Haskel, A.; Wang, J. Q.; Straub, T.; Neyroud, T. G.; Eisen, M. S. *J. Am. Chem. Soc.* **1999**, *121*, 3025.
(55) Wang, J. Q.; Eisen, M. S. *J. Organomet. Chem.* **2003**, *670*, 97.
(56) Korobkov, I.; Gambarotta, S.; Yap, G. P. A. *Organometallics* **2001**, *20*, 2552.
(57) Castro-Rodriguez, I.; Nakai, H.; Gantzel, P.; Zakharov, L. N.; Rheingold, A. L.; Meyer, K. *J. Am. Chem. Soc.* **2003**, *125*, 15734.
(58) Andrea, T.; Barnea, E.; Eisen, M. S. *J. Am. Chem. Soc.* **2008**, *130*, 245.
(59) Barnea, E.; Moradove, D.; Berthet, J.-C.; Ephritikhine, M.; Eisen, M. S. *Organometallics* **2006**, *25*, 320.
(60) Sharma, M.; Andrea, T.; Brookes, N. J.; Yates, B. F.; Eisen, M. S. *J. Am. Chem. Soc.* **2011**, *133*, 1341.
(61) Castro-Rodriguez, I.; Nakai, H.; Zakharov, L. N.; Rheingold, A. L.; Meyer, K. *Science* **2004**, *205*, 1757.
(62) Arunachalampillai, A.; Crewdson, P.; Korobkov, I.; Gambarotta, S. *Organometallics* **2006**, *25*, 3857.
(63) Roussel, P.; Scott, P. *J. Am. Chem. Soc.* **1998**, *120*, 1070.
(64) Fox, A. R.; Arnold, P. L.; Cummins, C. C. *J. Am. Chem. Soc.* **2010**, *132*, 3250.
(65) Jantunen, K. C.; Batchelor, R. J.; Leznoff, D. B. *Organometallics* **2004**, *23*, 2186.
(66) Jantunen, K. C.; Haftbaradaran, F.; Katz, M. J.; Batchelor, R. J.; Schatte, G.; Leznoff, D. B. *Dalton Trans.* **2005**, 3083.
(67) McCullough, L. G.; Turner, H. W.; Andersen, R. A.; Zalkin, A.; Templeton, D. H. *Inorg. Chem.* **1981**, *20*, 2869.
(68) Wilson, D. J.; Sebastian, A.; Cloke, F. G. N.; Avent, A. G.; Hitchcock, P. B. *Inorg. Chim. Acta* **2003**, *345*, 89.
(69) Patel, D.; Lewis, W.; Blake, A. J.; Liddle, S. T. *Dalton Trans.* **2010**, 6638.
(70) Hayes, C. E.; Leznoff, D. B. *Organometallics* **2010**, *29*, 767.
(71) Cruz, C. A.; Emslie, D. J. H.; Harrington, L. E.; Britten, J. F.; Robertson, C. M. *Organometallics* **2007**, *26*, 692.
(72) Fendrick, C. M.; Mintz, E. A.; Schertz, L. D.; Marks, T. J. *Organometallics* **1984**, *3*, 819.
(73) Bruno, J. W.; Smith, G. M.; Marks, T. J.; Fair, C. K.; Schultz, A. J.; Williams, J. M. *J. Am. Chem. Soc.* **1986**, *108*, 40.
(74) Shannon, R. D. *Acta Crystallogr., Sect. A: Found. Crystallogr.* **1976**, *32*, 751.
(75) Zhang, Z.; Schafer, L. L. *Org. Lett.* **2003**, *5*, 4733.
(76) Hermann, J. A.; Suttle, J. F. *Inorg. Synth.* **1957**, *5*, 143.
(77) Elias, A. J.; Roesky, H. W.; Robinson, W. T.; Sheldrick, G. M. *J. Chem. Soc., Dalton Trans.* **1993**, 495.
(78) Male, N. A. H.; Thornton-Pett, M.; Bochmann, M. *Dalton Trans.* **1997**, 2487.
(79) Leznoff, D. B.; Mund, G.; Jantunen, K. C.; Bhatia, P. H.; Gabert, A. J.; Batchelor, R. J. *J. Nucl. Sci. Technol.(Tokyo, Jpn.)* **2002**, *Suppl 3*, 406.
(80) Aizenberg, M.; Turculet, L.; Davis, W. M.; Schattenmann, F.; Schrock, R. R. *Organometallics* **1998**, *17*, 4795.
(81) Kondo, T.; Okada, T.; Mitsudo, T. *J. Am. Chem. Soc.* **2002**, *124*, 186.
(82) Gagne, M. R.; Stern, C. L.; Marks, T. J. *J. Am. Chem. Soc.* **1992**, *114*, 275.
(83) Riegert, D.; Collin, J.; Meddour, A.; Schulz, E.; Trifonov, A. *J. Org. Chem.* **2006**, *71*, 2514.
(84) Crimmin, M. R.; Arrowsmith, M.; Barrett, A. G. M.; Casely, I. J.; Hill, M. S.; Procopiou, P. A. *J. Am. Chem. Soc.* **2009**, *131*, 9670.
(85) Betteridge, P. W.; Carruthers, J. R.; Cooper, R. I.; Prout, K.; Watkin, D. J. *J. Appl. Crystallogr.* **2003**, *36*, 1487.
(86) Farrugia, L. J. *J. Appl. Crystallogr.* **1997**, *30*, 565.
(87) *Persistence of Vision Raytracer*, version 3.6.1; Persistence of Vision Pty. Ltd.: Williamstown, Victoria, Australia, 2004.